Ozone and DNA active UV radiation changes for the near global mean and at high latitudes due to enhanced greenhouse gas concentrations

Kostas Eleftheratos[1,2], John Kapsomenakis[3], Ilias Fountoulakis[4,5], Christos S. Zerefos[2,3,6], Patrick Jöckel[7], Martin Dameris[7], Alkiviadis F. Bais[8], Germar Bernhard[9], Dimitra Kouklaki[1], Kleareti Tourpali[8], Scott Stierle[10], J. Ben Liley[11], Colette Brogniez[12], Frédérique Auriol[12], Henri Diémoz[5], Stana Simic[13], Irina Petropavlovskikh[14]

[1]Department of Geology and Geoenvironment, National and Kapodistrian University of Athens, Athens, Greece
[2]Center for Environmental Effects on Health, Biomedical Research Foundation of the Academy of Athens, Athens, Greece
[3]Research Centre for Atmospheric Physics and Climatology, Academy of Athens, Athens, Greece
[4]Institute for Astronomy, Astrophysics, Space Applications and Remote Sensing, National Observatory of Athens (IAASARS/NOA), Athens, Greece
[5]Aosta Valley Regional Environmental Protection Agency (ARPA), Saint-Christophe, Italy
[6]Navarino Environmental Observatory (N.E.O), Messenia, Greece
[7]Deutsches Zentrum für Luft- und Raumfahrt, Institut für Physik der Atmosphäre, Oberpfaffenhofen, Germany
[8]Department of Physics, Aristotle University of Thessaloniki, Thessaloniki, Greece
[9]Biospherical Instruments Inc., San Diego, CA 92110, USA
[10]NOAA Global Monitoring Laboratory, Boulder, CO 80305, USA
[11]National Institute of Water & Atmospheric Research (NIWA), Lauder, New Zealand
[12]Univ. Lille, CNRS, UMR 8518 - Laboratoire d'Optique Atmosphérique, F-59000 Lille, France
[13]Institute for Meteorology and Climatology, University of Natural Resources and Life Sciences, Vienna 1180, Austria
[14]Cooperative Institute for Research in Environmental Sciences, University of Colorado, Boulder, CO, USA

Correspondence to: Kostas Eleftheratos (kelef@geol.uoa.gr)

Table S1. Statistics of correlations between modelled (EMAC CCM "specified dynamics" simulation SC1SD-base-02) and observed (ground-based) DNA active irradiance data after removing variability related to the seasonal cycle. Stations are listed from north to south.

Station	Latitude	Correlation	Intercept (%)	Slope	Error	t-value	p-value	N
Summit, Greenland	72.58	0.70942	-0.63182	0.75691	0.08109	9.33455	<0.0001	88
Barrow, AK, United States	71.32	0.34199	0.23804	0.68041	0.18074	3.76456	2.72957E-4	109
Villeneuve d'Ascq, France	50.61	0.69524	-0.7477	0.87007	0.07089	12.27297	<0.0001	163
Groß-Enzersdorf, Austria	48.20	0.58206	-1.04209	0.64811	0.06711	9.65676	<0.0001	184
Zugspitze, Germany	47.42	0.2659	1.13542	0.2448	0.1281	1.91101	0.06198	50
Hoher Sonnblick, Austria	47.05	0.67287	1.11524	0.94558	0.07542	12.53774	<0.0001	192
Aosta, Italy	45.74	0.67091	-1.23967	1.33004	0.14016	9.48924	<0.0001	112
Observatoire de Haute Provence, France	43.94	0.57419	-2.10876	0.72899	0.10447	6.97814	<0.0001	101
Thessaloniki, Greece	40.63	0.61157	-0.65425	0.76343	0.06984	10.93159	<0.0001	202
Boulder, CO, United States	39.99	0.74751	0.19874	0.67683	0.0474	14.2792	<0.0001	163
Athens, Greece	37.99	0.46825	-1.20784	0.31889	0.05141	6.20271	<0.0001	139
Mauna Loa, HI, United States	19.53	0.57692	0.35833	0.50906	0.04962	10.25995	<0.0001	213
Reunion Island, St. Denis, France	-20.90	0.29475	-0.01221	0.23706	0.09532	2.48686	0.01546	67
Alice Springs, Australia	-23.80	0.59268	-0.13242	0.60587	0.0691	8.7686	<0.0001	144
Lauder, New Zealand	-45.04	0.52901	0.08797	0.84026	0.09301	9.03374	<0.0001	212
Ushuaia, Argentina	-54.82	0.44285	-0.63202	0.79185	0.21234	3.72909	4.44141E-4	59
Palmer, Antarctica	-64.77	0.4665	-0.09991	0.71651	0.12103	5.92008	<0.0001	128
Arrival Heights, Antarctica	-77.83	0.93868	0.53114	0.99985	0.03298	30.31727	<0.0001	126
South Pole, Antarctica	-90	0.94832	-0.20478	1.04666	0.03238	32.32625	<0.0001	119

Table S2. Statistics of correlations between modelled (EMAC CCM "specified dynamics" simulation SC1SD-base-02) and observed (satellite SBUV v8.7) total ozone data after removing variability related to the seasonal cycle. Stations are listed from north to south.

Station	Latitude	Correlation	Intercept (%)	Slope	Error	t-value	p-value	N
Summit, Greenland	72.58	0.92746	0.02356	0.79136	0.02809	28.17083	<0.0001	131
Barrow, AK, United States	71.32	0.91395	-0.07433	0.89544	0.03501	25.57902	<0.0001	131
Villeneuve d'Ascq, France	50.61	0.9327	0.00865	0.8832	0.02297	38.44502	<0.0001	223
Groß-Enzersdorf, Austria	48.20	0.90117	-2.71279E-4	0.83541	0.02703	30.90677	<0.0001	223
Zugspitze, Germany	47.42	0.90637	-0.00303	0.81468	0.02554	31.89276	<0.0001	223
Hoher Sonnblick, Austria	47.05	0.90234	-0.00193	0.80291	0.0258	31.12256	<0.0001	223
Aosta, Italy	45.74	0.90909	-0.00663	0.85712	0.02642	32.44056	<0.0001	223
Observatoire de Haute Provence, France	43.94	0.90651	-0.01346	0.86718	0.02717	31.9194	<0.0001	223
Thessaloniki, Greece	40.63	0.84905	-0.00866	0.79992	0.03348	23.89163	<0.0001	223
Boulder, CO, United States	39.99	0.85389	-0.00778	0.75677	0.03103	24.38992	<0.0001	223
Athens, Greece	37.99	0.84712	-0.01027	0.84485	0.03565	23.69841	<0.0001	223
Mauna Loa, HI, United States	19.53	0.85221	-0.05717	0.94063	0.03885	24.21468	<0.0001	223
Reunion Island, St. Denis, France	-20.90	0.76869	0.00266	0.80808	0.04523	17.8657	<0.0001	223
Alice Springs, Australia	-23.80	0.85137	0.00285	0.85687	0.03551	24.12727	<0.0001	223
Lauder, New Zealand	-45.04	0.92117	0.03962	0.87216	0.02479	35.18816	<0.0001	223
Ushuaia, Argentina	-54.82	0.96269	0.01129	0.86996	0.02179	39.93037	<0.0001	128
Palmer, Antarctica	-64.77	0.95377	-0.10395	0.89986	0.02526	35.6213	<0.0001	128
Arrival Heights, Antarctica	-77.83	0.89556	-0.13406	0.65541	0.02901	22.59306	<0.0001	128
South Pole, Antarctica	-90	no data	no data	no data	no data	no data	no data	no data

Table S3. Statistics of correlations between modelled (EMAC CCM "specified dynamics" simulation SC1SD-base-02) and observed (satellite MODIS/Terra) cloudiness data after removing variability related to the seasonal cycle. Stations are listed from north to south.

Station	Latitude	Correlation	Intercept (%)	Slope	Error	t-value	p-value	N
Summit, Greenland	72.58	0.19614	0.01033	0.06936	0.03053	2.2719	0.02475	131
Barrow, AK, United States	71.32	0.59746	0.01835	0.75521	0.08925	8.46216	<0.0001	131
Villeneuve d'Ascq, France	50.61	0.5155	-0.0936	0.50165	0.05622	8.92306	<0.0001	222
Groß-Enzersdorf, Austria	48.20	0.65362	-0.15377	0.61759	0.04821	12.80986	<0.0001	222
Zugspitze, Germany	47.42	0.54779	-0.02613	0.57172	0.05887	9.71188	<0.0001	222
Hoher Sonnblick, Austria	47.05	0.55629	-0.04129	0.61867	0.06231	9.92925	<0.0001	222
Aosta, Italy	45.74	0.66827	-0.06953	0.68816	0.05165	13.3242	<0.0001	222
Observatoire de Haute Provence, France	43.94	0.44998	-0.07471	0.45353	0.06068	7.4736	<0.0001	222
Thessaloniki, Greece	40.63	0.64131	-0.8916	0.86816	0.07084	12.2556	<0.0001	217
Boulder, CO, United States	39.99	0.53923	-0.09291	0.48194	0.05075	9.49717	<0.0001	222
Athens, Greece	37.99	0.48522	-1.26658	0.68926	0.08592	8.02237	<0.0001	211
Mauna Loa, HI, United States	19.53	0.592	-1.20988	1.35496	0.1258	10.77071	<0.0001	217
Reunion Island, St. Denis, France	-20.90	0.52781	-1.53877	1.18482	0.12943	9.15397	<0.0001	219
Alice Springs, Australia	-23.80	0.62268	-0.25621	0.58451	0.05233	11.16931	<0.0001	199
Lauder, New Zealand	-45.04	0.3935	0.07335	0.45073	0.071	6.34872	<0.0001	222
Ushuaia, Argentina	-54.82	0.44364	-0.09417	0.60317	0.10855	5.55661	<0.0001	128
Palmer, Antarctica	-64.77	0.47323	0.00415	0.55019	0.09124	6.02995	<0.0001	128
Arrival Heights, Antarctica	-77.83	0.53671	0.28879	0.94892	0.1329	7.14	<0.0001	129
South Pole, Antarctica	-90	-0.17482	-0.14172	-0.04717	0.02467	-1.91231	0.0583	118

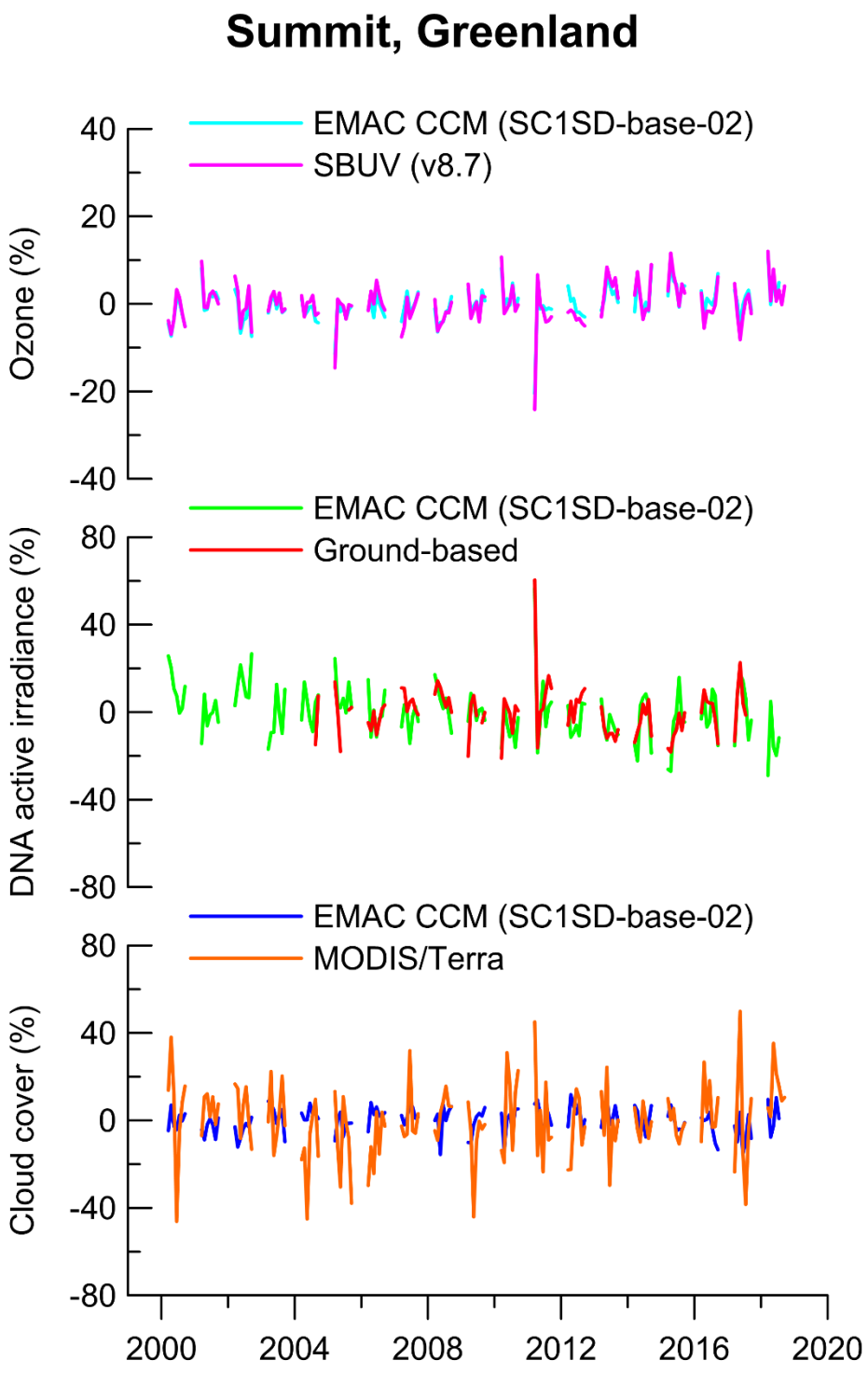
Summit, Greenland
EMAC CCM (SC1SD-base-02)
SBUV (v8.7)
Ozone (%)
40
20
0
-20
-40
EMAC CCM (SC1SD-base-02)
Ground-based
DNA active irradiance (%)
80
40
0
-40
-80
EMAC CCM (SC1SD-base-02)
MODIS/Terra
Cloud cover (%)
80
40
0
-40
-80
2000
2004
2008
2012
2016
2020

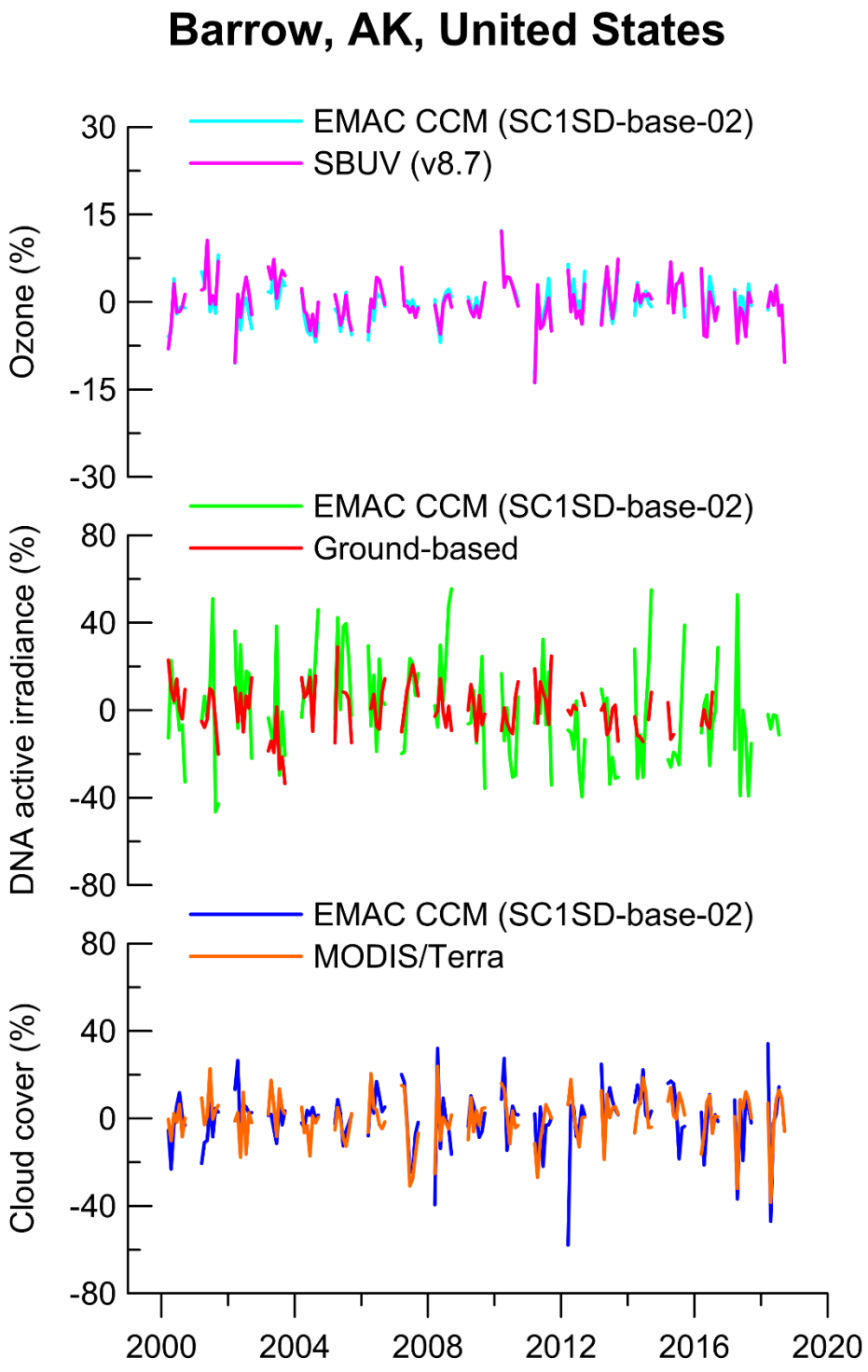
Barrow, AK, United States
EMAC CCM (SC1SD-base-02)
SBUV (v8.7)
Ozone (%)
30
15
0
-15
-30
EMAC CCM (SC1SD-base-02)
Ground-based
DNA active irradiance (%)
80
40
0
-40
-80
EMAC CCM (SC1SD-base-02)
MODIS/Terra
Cloud cover (%)
80
40
0
-40
-80
2000
2004
2008
2012
2016
2020

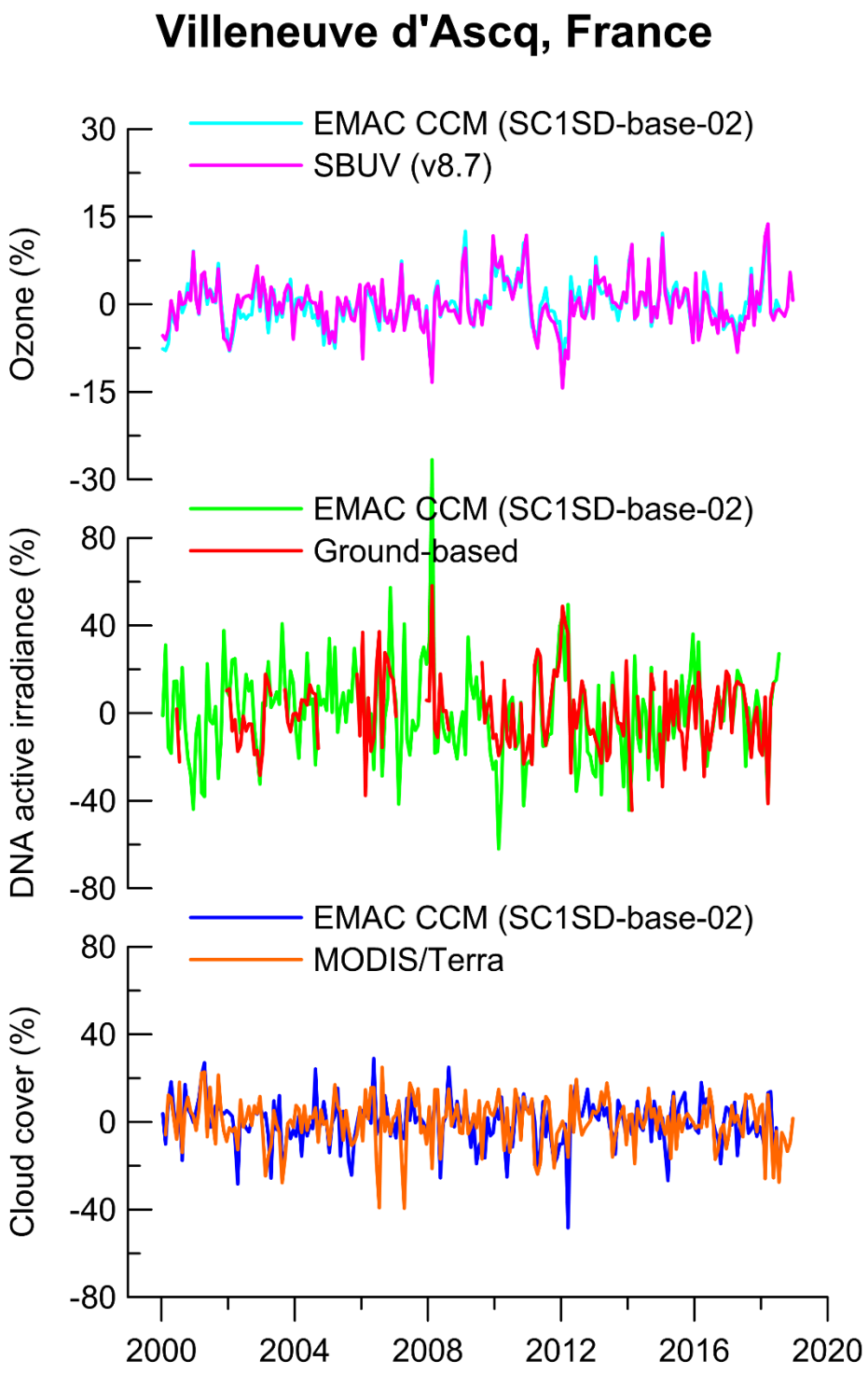
Villeneuve d'Ascq, France
EMAC CCM (SC1SD-base-02)
SBUV (v8.7)
Ozone (%)
30
15
0
-15
-30
EMAC CCM (SC1SD-base-02)
Ground-based
DNA active irradiance (%)
80
40
0
-40
-80
EMAC CCM (SC1SD-base-02)
MODIS/Terra
Cloud cover (%)
80
40
0
-40
-80
2000
2004
2008
2012
2016
2020

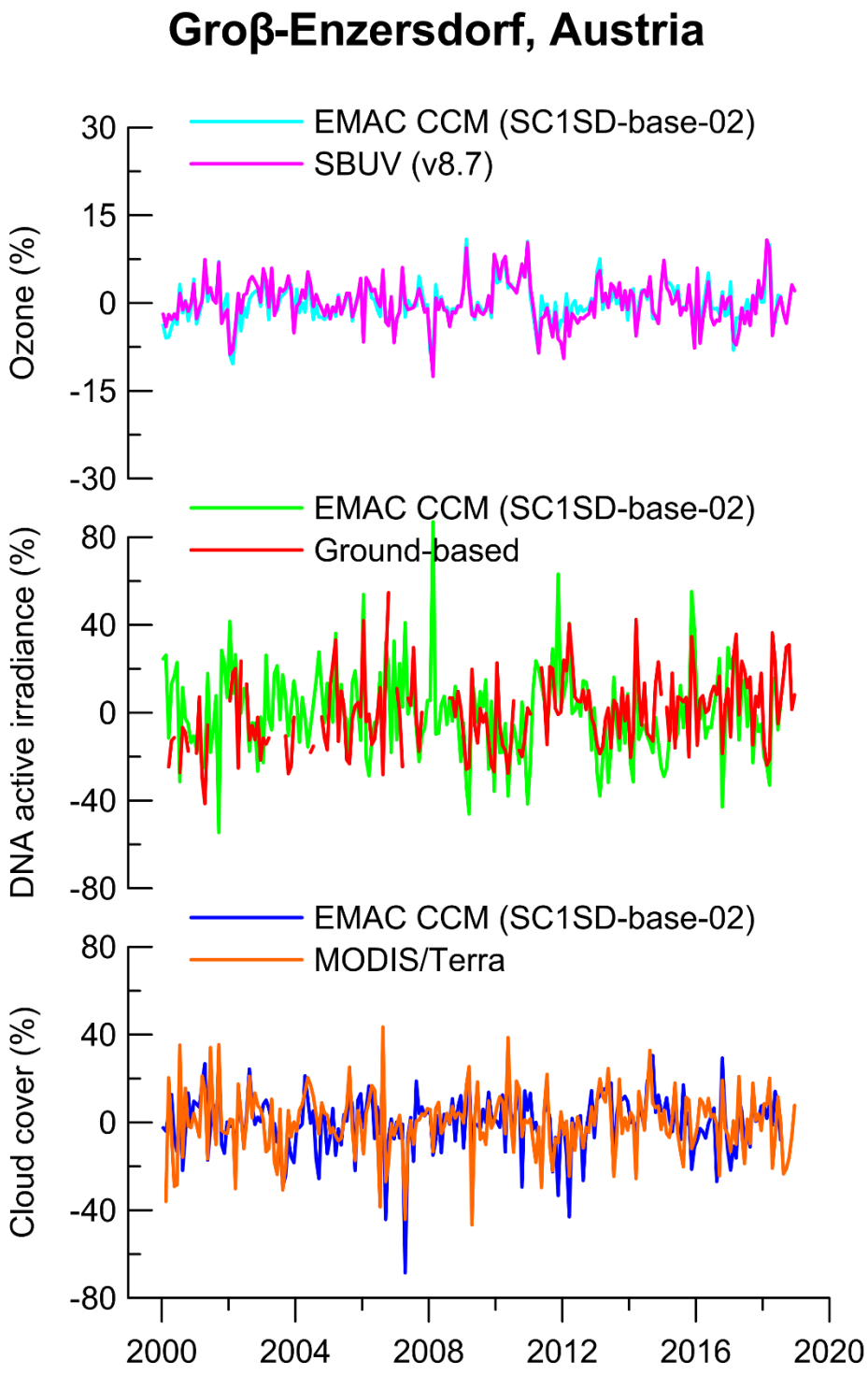
Groß-Enzersdorf, Austria
EMAC CCM (SC1SD-base-02)
SBUV (v8.7)
Ozone (%)
30
15
0
-15
-30
EMAC CCM (SC1SD-base-02)
Ground-based
DNA active irradiance (%)
80
40
0
-40
-80
EMAC CCM (SC1SD-base-02)
MODIS/Terra
Cloud cover (%)
80
40
0
-40
-80
2000
2004
2008
2012
2016
2020

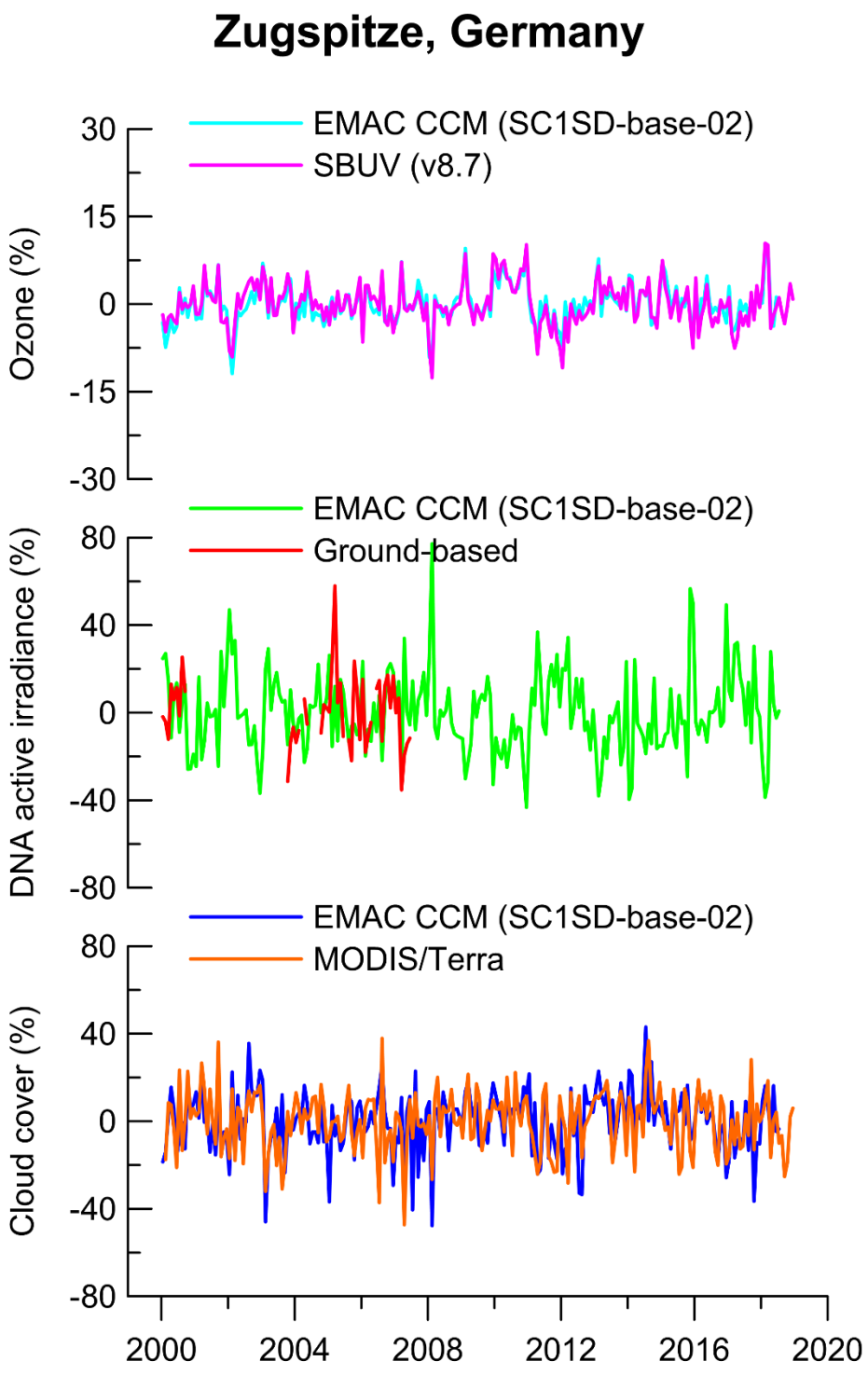
Zugspitze, Germany
EMAC CCM (SC1SD-base-02)
SBUV (v8.7)
Ozone (%)
30
15
0
-15
-30
EMAC CCM (SC1SD-base-02)
Ground-based
DNA active irradiance (%)
80
40
0
-40
-80
EMAC CCM (SC1SD-base-02)
MODIS/Terra
Cloud cover (%)
80
40
0
-40
-80
2000
2004
2008
2012
2016
2020

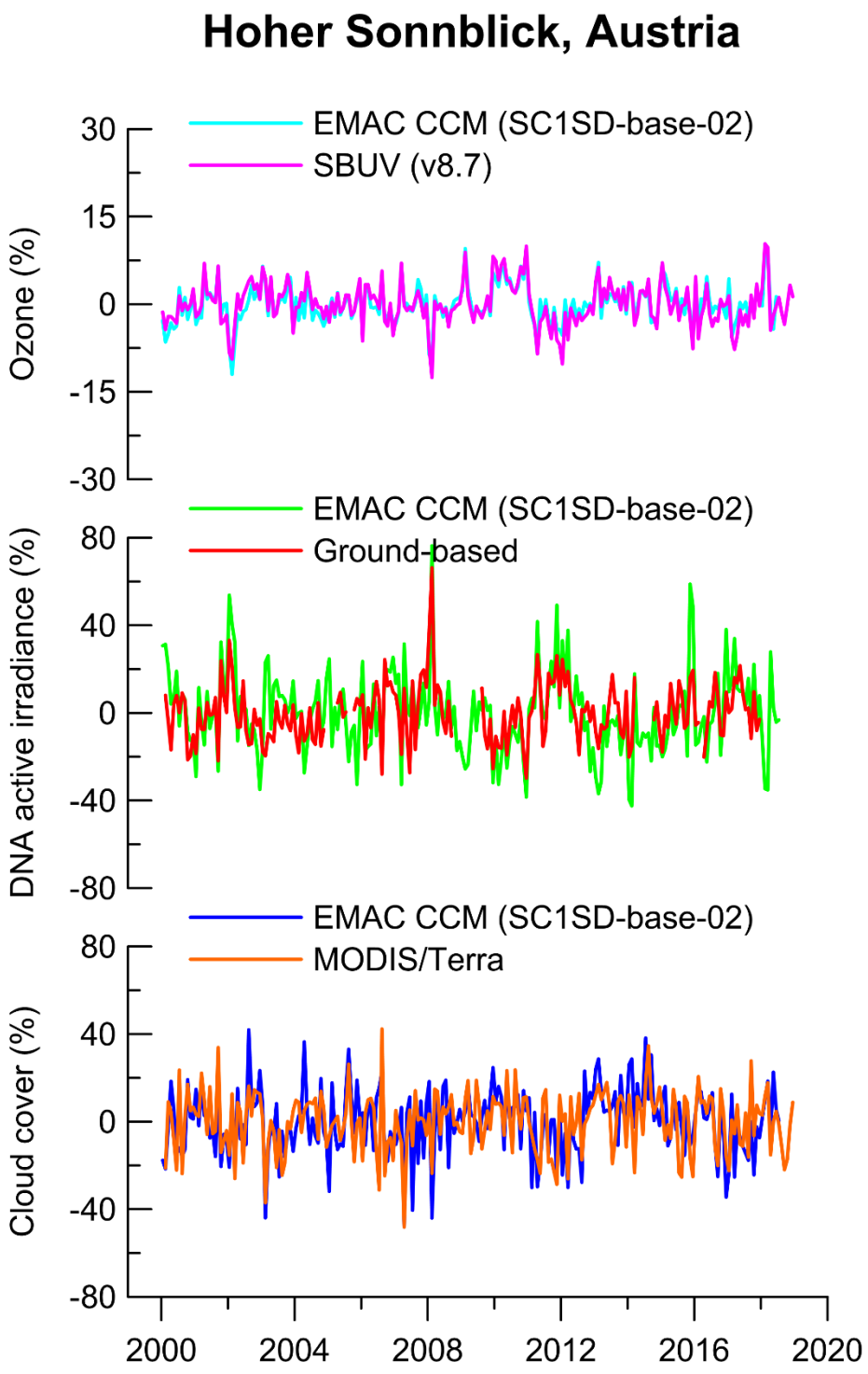
Hoher Sonnblick, Austria
EMAC CCM (SC1SD-base-02)
SBUV (v8.7)
Ozone (%)
30
15
0
-15
-30
EMAC CCM (SC1SD-base-02)
Ground-based
DNA active irradiance (%)
80
40
0
-40
-80
EMAC CCM (SC1SD-base-02)
MODIS/Terra
Cloud cover (%)
80
40
0
-40
-80
2000
2004
2008
2012
2016
2020

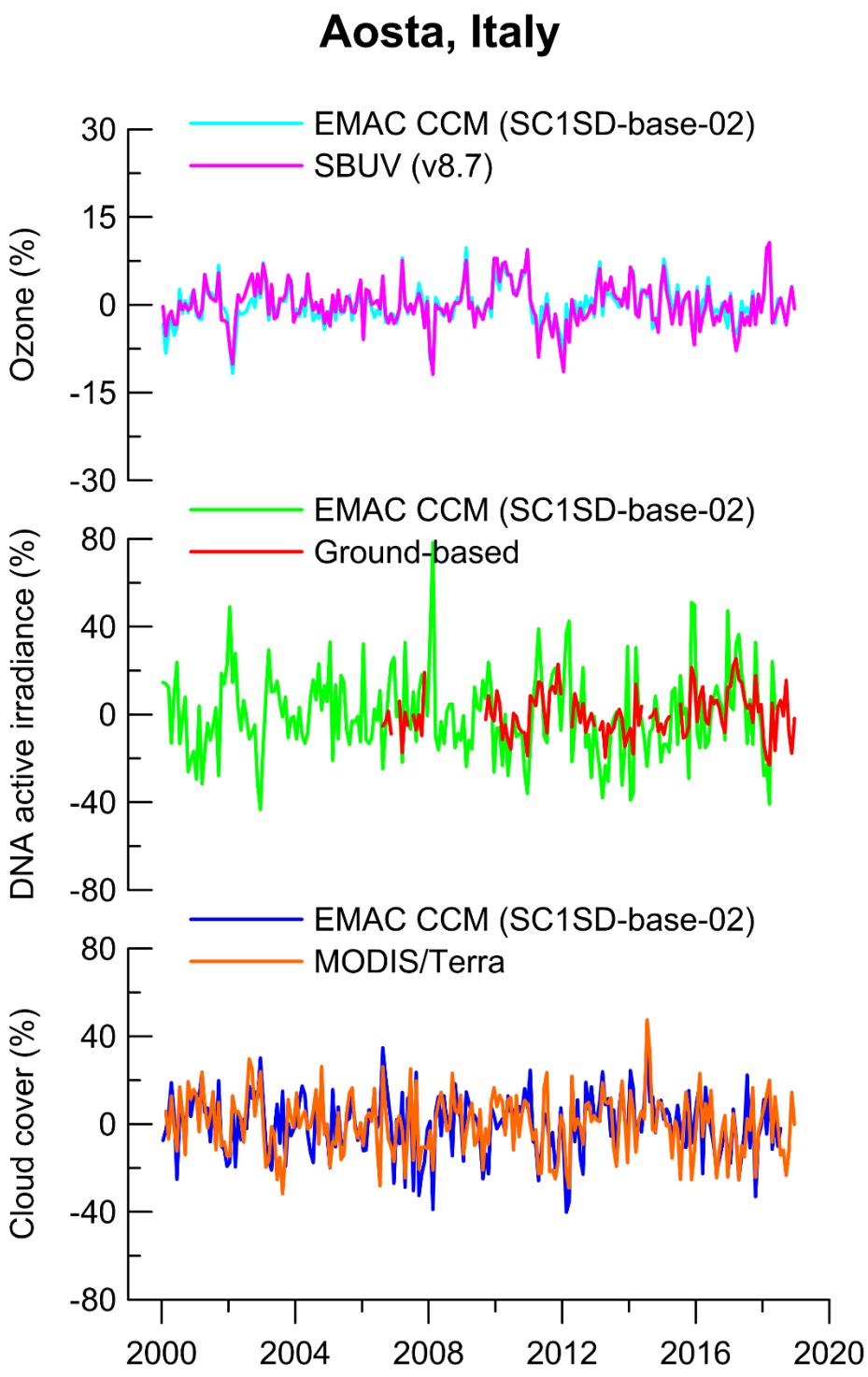
Aosta, Italy
EMAC CCM (SC1SD-base-02)
SBUV (v8.7)
Ozone (%)
30
15
0
-15
-30
EMAC CCM (SC1SD-base-02)
Ground-based
DNA active irradiance (%)
80
40
0
-40
-80
EMAC CCM (SC1SD-base-02)
MODIS/Terra
Cloud cover (%)
80
40
0
-40
-80
2000
2004
2008
2012
2016
2020

Observatoire de Haute Provence, France

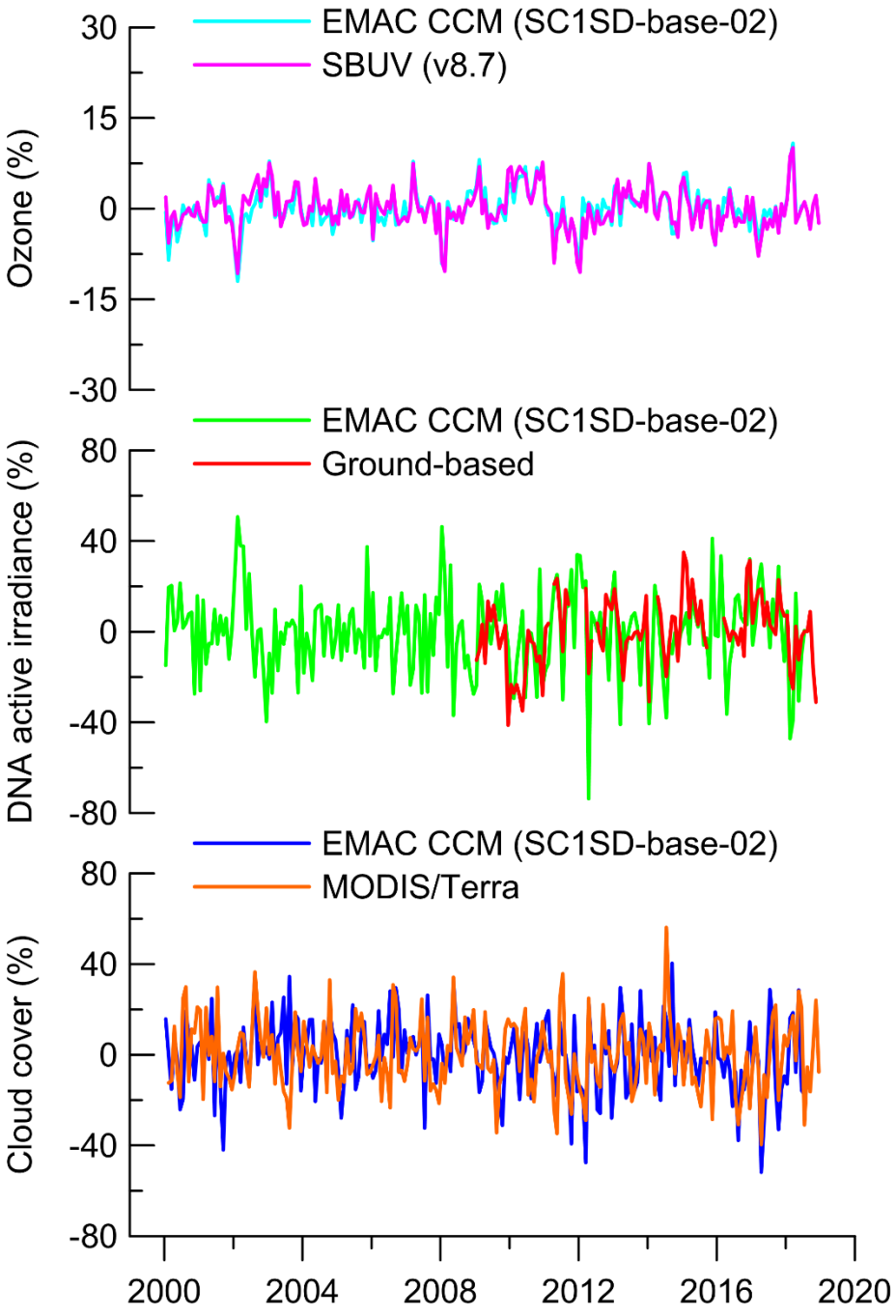

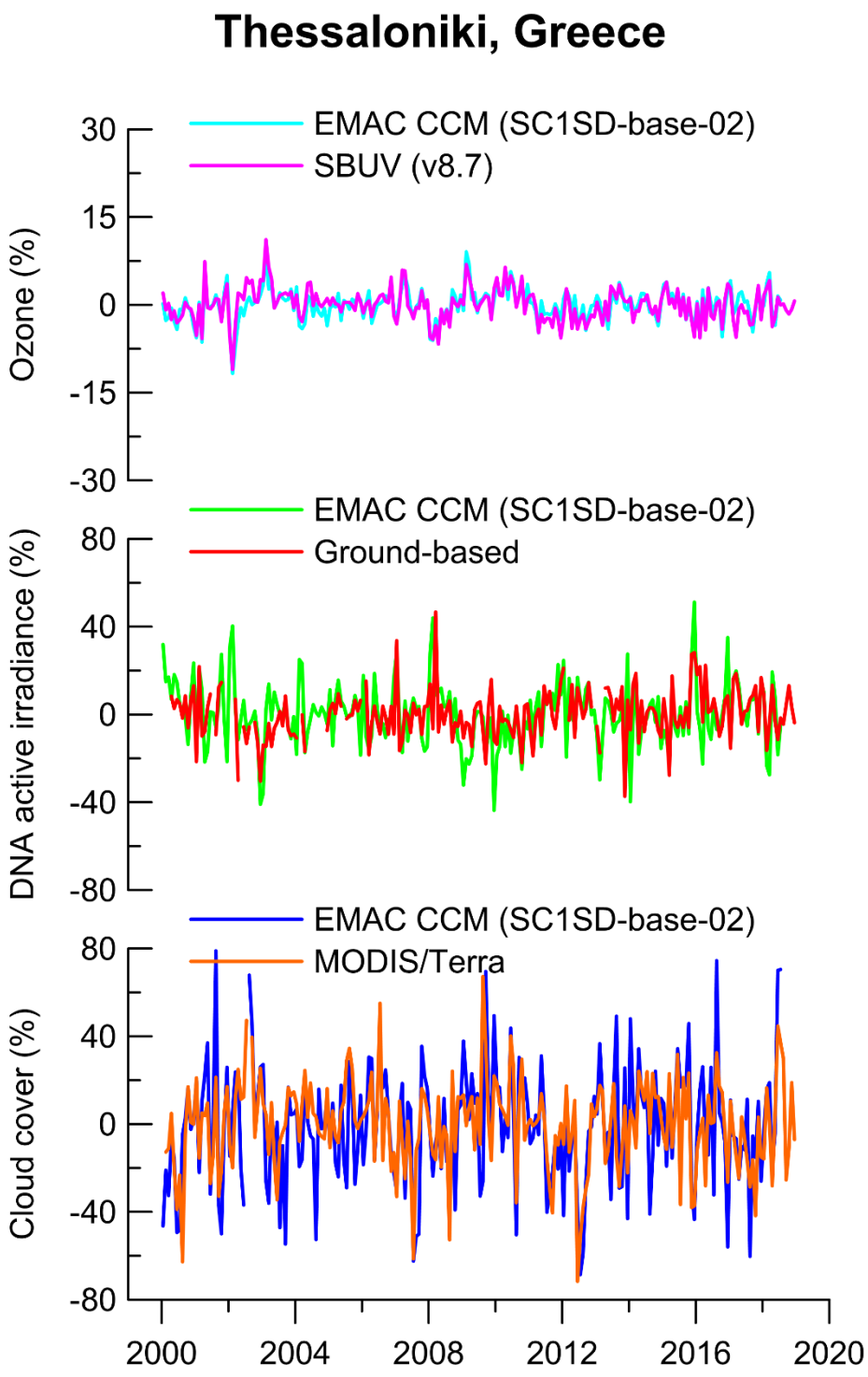
Thessaloniki, Greece
EMAC CCM (SC1SD-base-02)
SBUV (v8.7)
Ozone (%)
30
15
0
-15
-30
EMAC CCM (SC1SD-base-02)
Ground-based
DNA active irradiance (%)
80
40
0
-40
-80
EMAC CCM (SC1SD-base-02)
MODIS/Terra
Cloud cover (%)
80
40
0
-40
-80
2000
2004
2008
2012
2016
2020

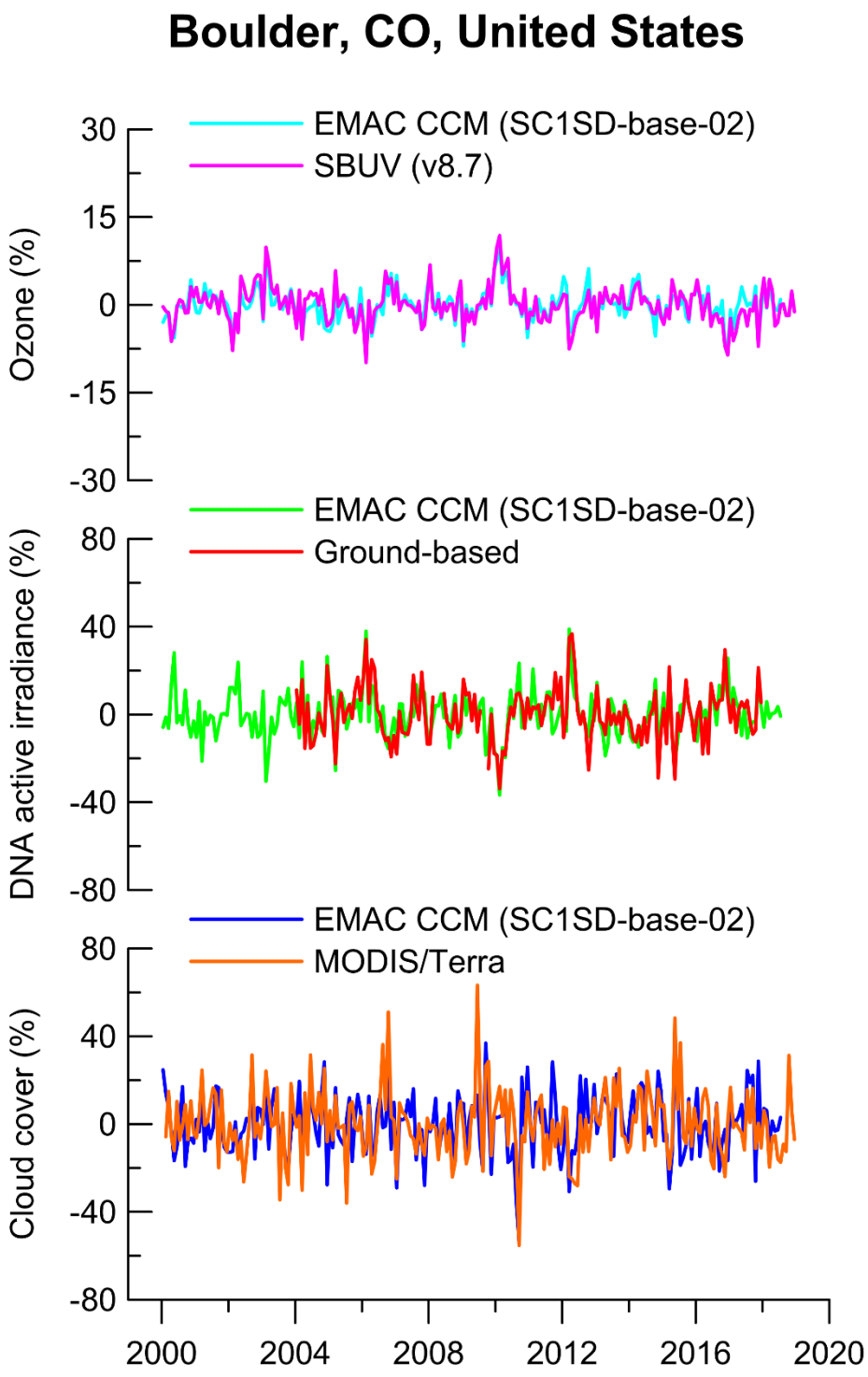
Boulder, CO, United States
EMAC CCM (SC1SD-base-02)
SBUV (v8.7)
Ozone (%)
30
15
0
-15
-30
EMAC CCM (SC1SD-base-02)
Ground-based
DNA active irradiance (%)
80
40
0
-40
-80
EMAC CCM (SC1SD-base-02)
MODIS/Terra
Cloud cover (%)
80
40
0
-40
-80
2000
2004
2008
2012
2016
2020

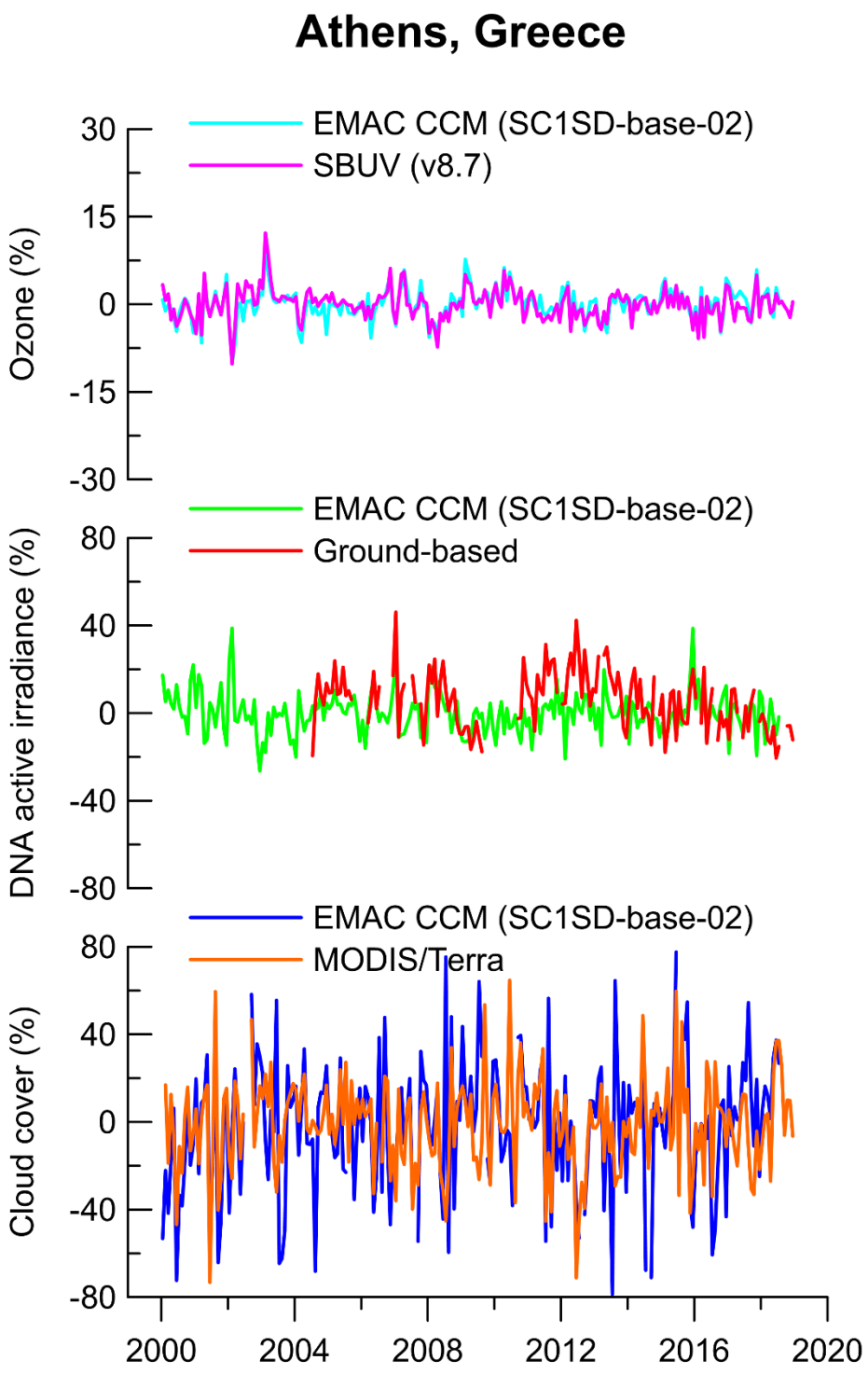
Athens, Greece
EMAC CCM (SC1SD-base-02)
SBUV (v8.7)
Ozone (%)
30
15
0
-15
-30
EMAC CCM (SC1SD-base-02)
Ground-based
DNA active irradiance (%)
80
40
0
-40
-80
EMAC CCM (SC1SD-base-02)
MODIS/Terra
Cloud cover (%)
80
40
0
-40
-80
2000
2004
2008
2012
2016
2020

Mauna Loa, HI, United States

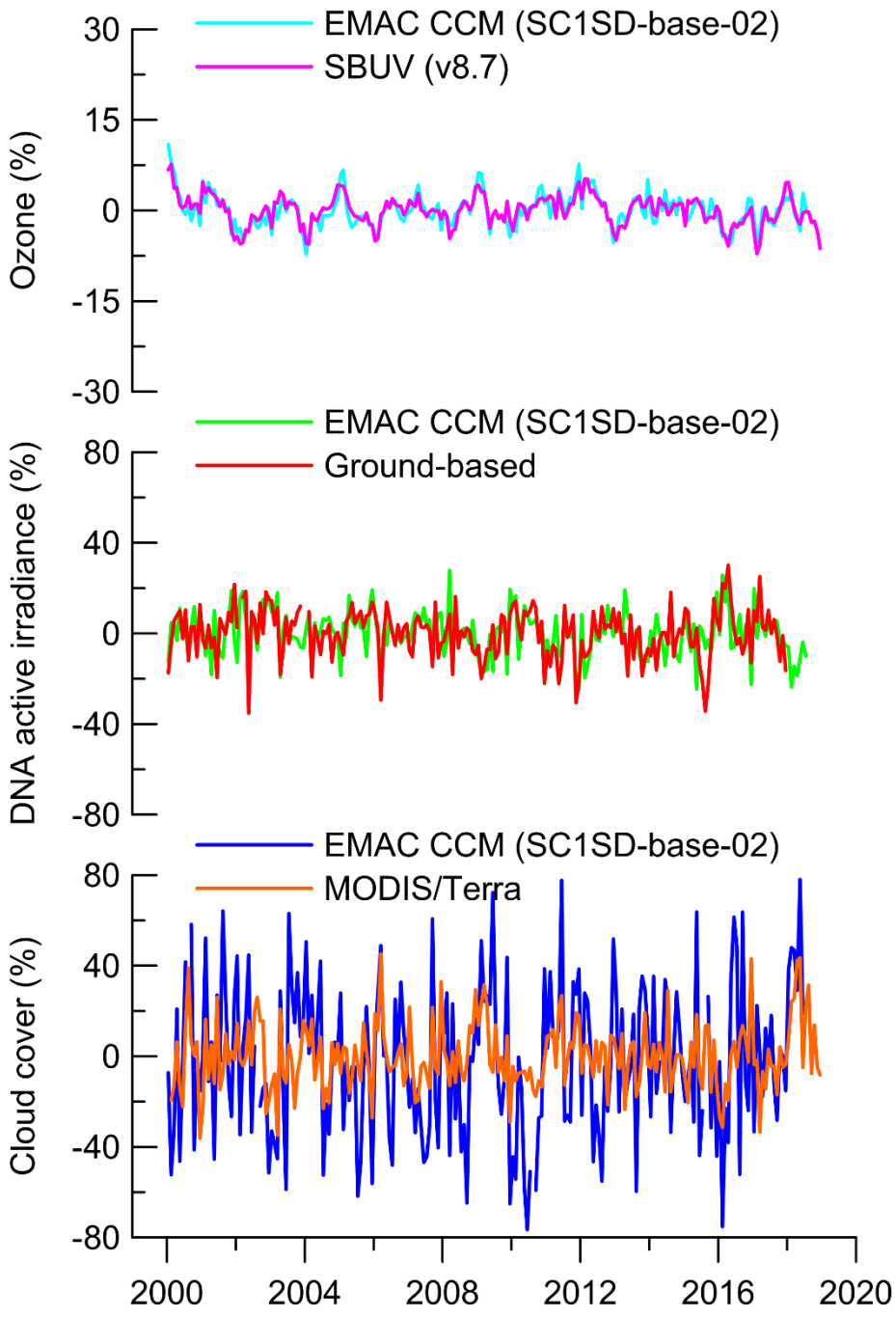

Reunion Island, St. Denis, France

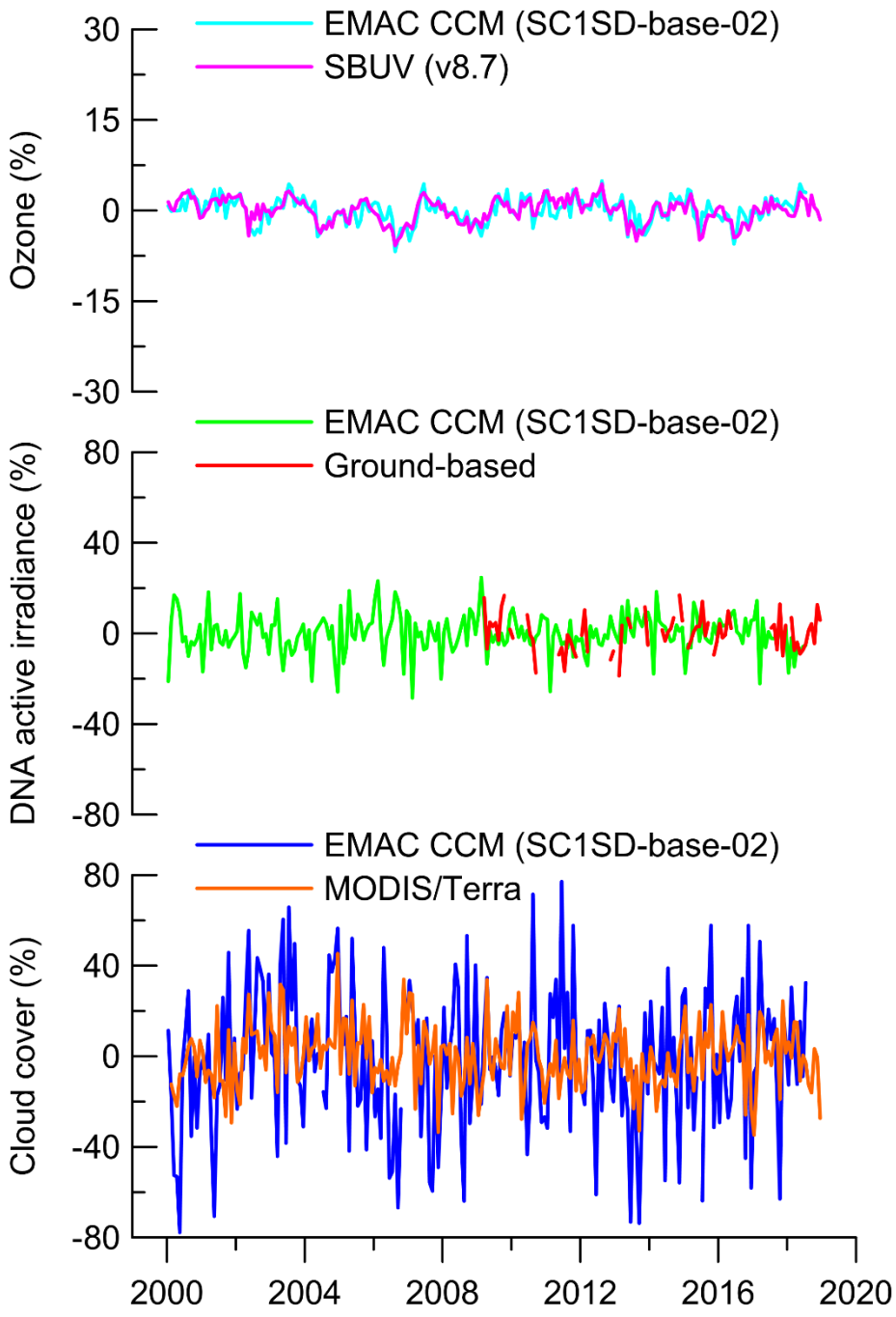

Alice Springs, Australia

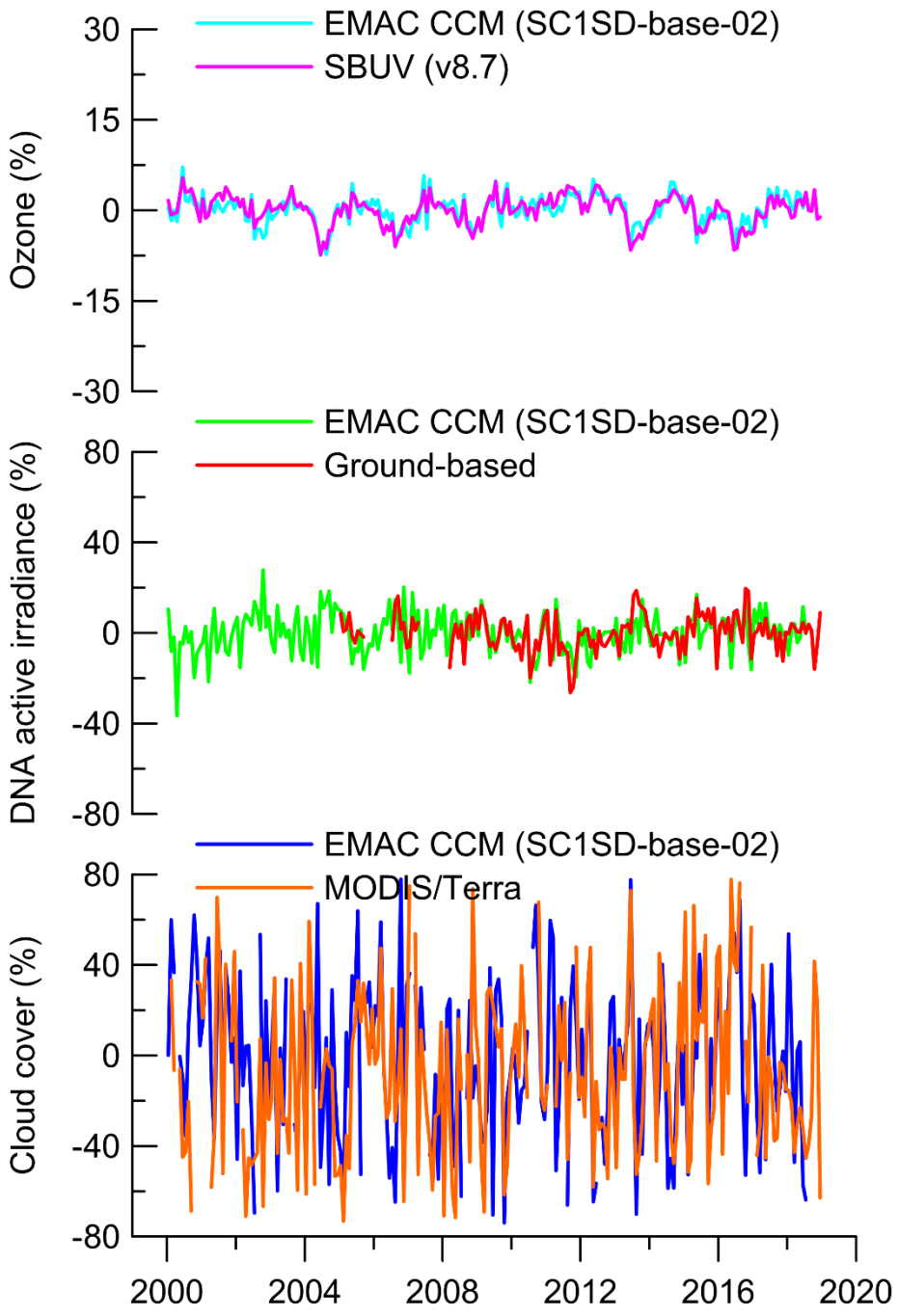

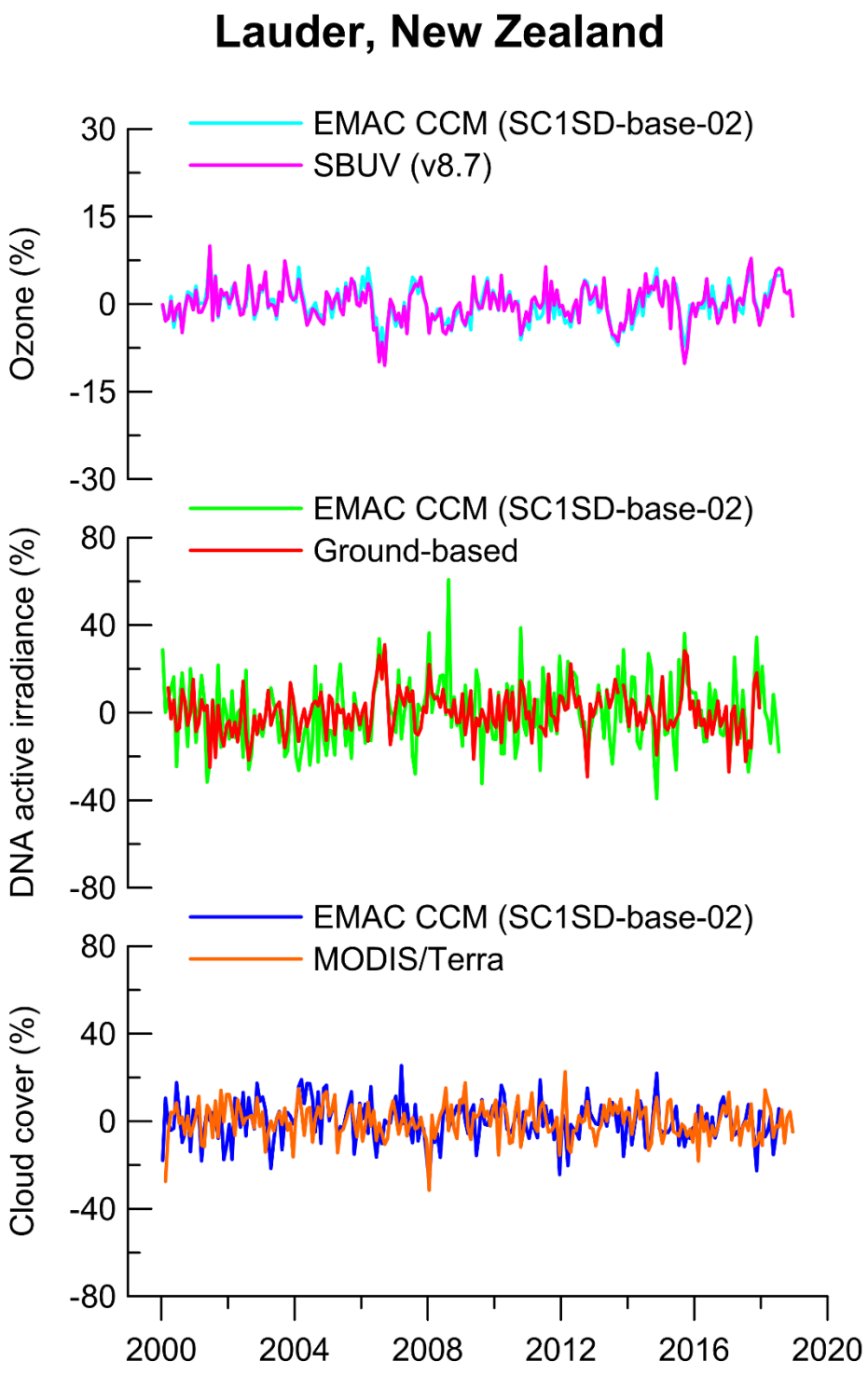
Lauder, New Zealand
EMAC CCM (SC1SD-base-02)
SBUV (v8.7)
Ozone (%)
30
15
0
-15
-30
EMAC CCM (SC1SD-base-02)
Ground-based
DNA active irradiance (%)
80
40
0
-40
-80
EMAC CCM (SC1SD-base-02)
MODIS/Terra
Cloud cover (%)
80
40
0
-40
-80
2000
2004
2008
2012
2016
2020

Ushuaia, Argentina

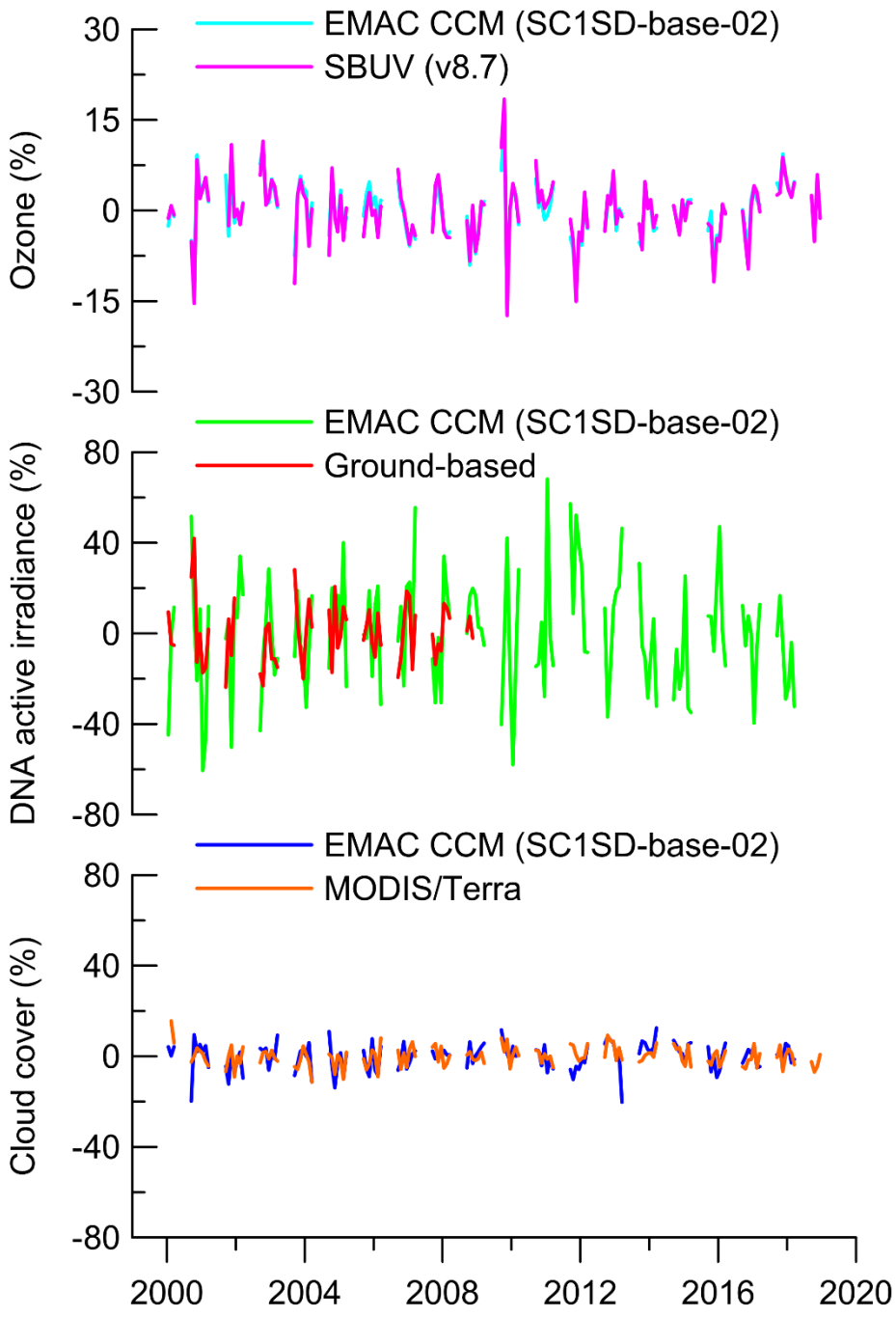

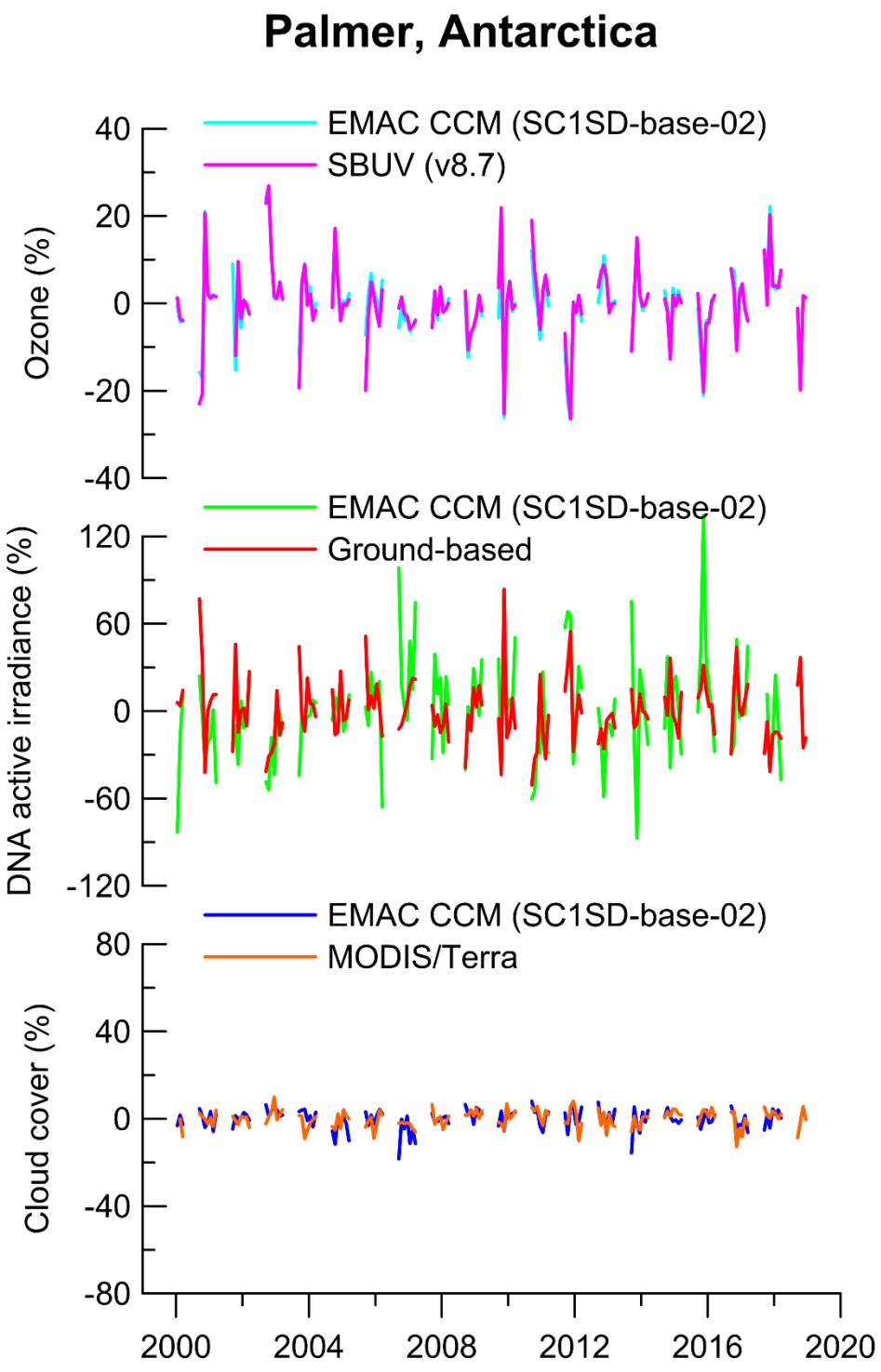
Palmer, Antarctica
EMAC CCM (SC1SD-base-02)
SBUV (v8.7)
Ozone (%)
40
20
0
-20
-40
EMAC CCM (SC1SD-base-02)
Ground-based
DNA active irradiance (%)
120
60
0
-60
-120
EMAC CCM (SC1SD-base-02)
MODIS/Terra
Cloud cover (%)
80
40
0
-40
-80
2000
2004
2008
2012
2016
2020

Arrival Heights, Antarctica

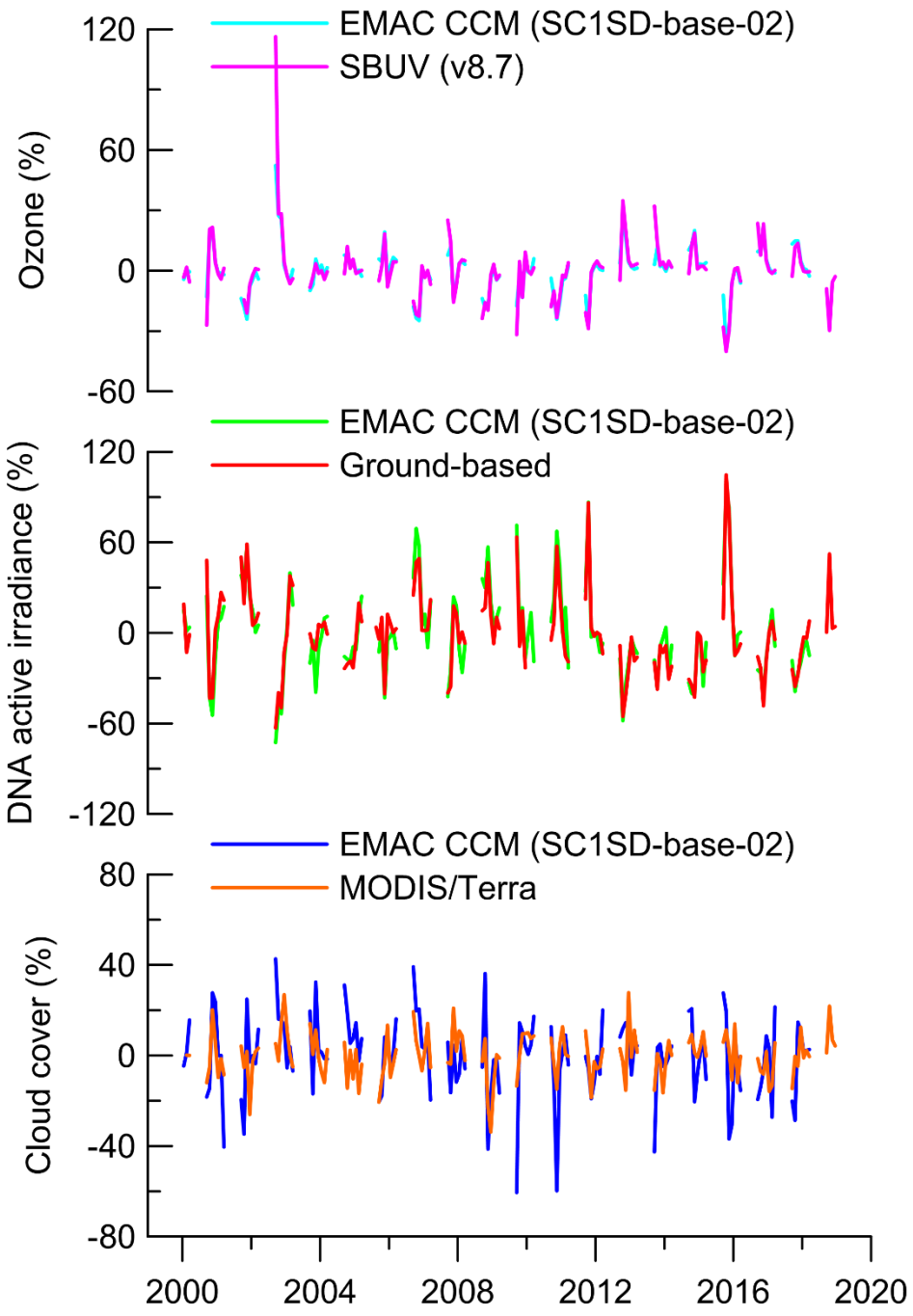

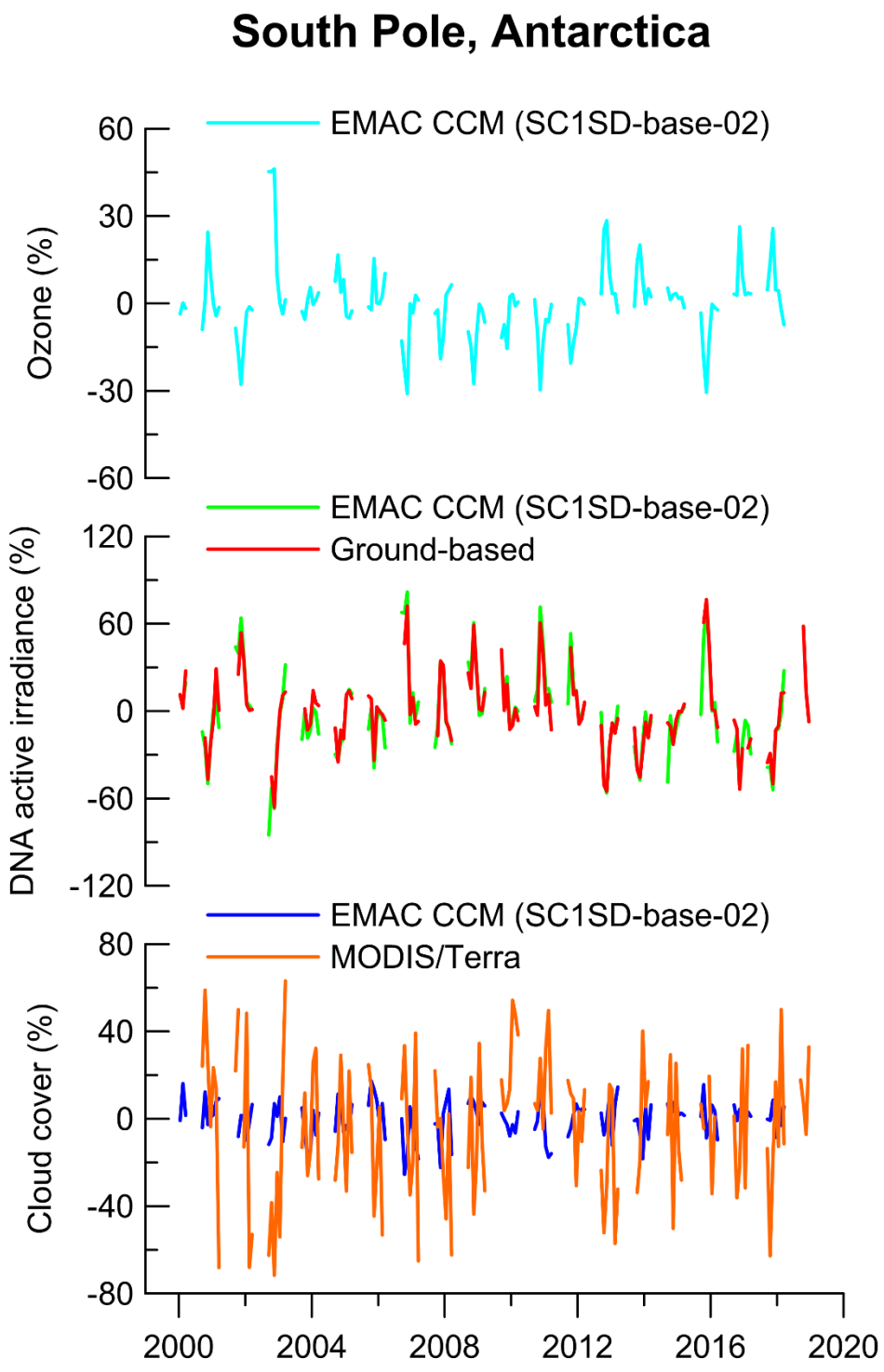
South Pole, Antarctica
EMAC CCM (SC1SD-base-02)
Ozone (%)
60
30
0
-30
-60
EMAC CCM (SC1SD-base-02)
Ground-based
DNA active irradiance (%)
120
60
0
-60
-120
EMAC CCM (SC1SD-base-02)
MODIS/Terra
Cloud cover (%)
80
40
0
-40
-80
2000
2004
2008
2012
2016
2020